The structure of sedimentary basins of Antarctica and a new three-layer sediment model

A. Baranov [1], A. Morelli [2]

[1] Schmidt Institute of Physics of the Earth, Russian Academy of Sciences, Moscow, Russia.

[2] Istituto Nazionale di Geofisica e Vulcanologia, Sezione di Bologna, via Donato Creti 12, 40128 Bologna, Italy.

Corresponding Author address

Email: aabaranov@gmail.com

Abstract:

We use geophysical data together with a recent subglacial bedrock map (BEDMACHINE model) to obtain and investigate a new three-layer sediment model for Antarctica that substantially improves the knowledge of global sediment distribution. We also provide a combined, continuous, sediment model for Antarctica and surrounding oceans by joining such improved continental sedimentary model with an existing global one (GlobSed). Our results reveal large differences between sedimentary basins for Antarctica as a function of their age and origin. The maximum thickness of sediments is reached under Filchner-Ronne Ice Shelf and off the Weddell Sea coast (10-12 km) Further offshore, towards the ocean, the thickness of sediments drops to 4-5 km. As often done, we also divide the sediment cover in three layers to distinguish material with different properties. The lower sediment layer (deeper than 7 km) with high P-wave velocities (4.0-4.9 km/s) is found only for Lambert Rift and Filchner-Ronne basin. The middle layer (2-7 km) has large variations for different sedimentary basins: 3.5-3.7 km/s for Lambert, Basin; 4.0-4.3 km/s for Ross, Byrd and

Bentley basins; 3.3-4.0 km/s for Filchner-Ronne basin. The upper sediment layer (0-2 km) has large velocity variations, from 2.0 km/s for Ross and Lambert basins (young sediments) to 4.7 km/s for Dronning Maud Land basins. We suggest that P-wave velocity larger than 4 km/s represents old, compacted sediments which belong to the Beacon Supergroup; about 3 km/s refers to Mesozoic (rifted?) sediments; and less than 3 km/s relates to young Cenozoic sediments. According to this criterion, Pensacola-Pole, Dronning Maud Land, Bentley and Byrd basins belong to the Beacon Supergroup, while more complex and thicker Ross, Lambert and Filchner-Ronne basins contain sediments from Beacon Supergroup in the middle or lower layer, respectively. Other sedimentary basins with more moderate velocities possibly belong to the East Antarctic Rift System which formed later during Gondwana breakup.

Key words: sediment structure, Antarctica, Gondwana, Beacon Supergroup, GlobSed, ANTASed.

1. Introduction

Sediments form a very heterogeneous, and highly varying in thickness, layer of the Earth, that could mask the signature of deeper structure in potential fields, making it more difficult to retrieve. Globally, the thickness of the sediments varies from 0 to more than 20 km (Laske and Masters, 1997). The properties of sediments vary greatly depending on their history and type of sedimentation. In addition, the study of sedimentation provides insight into the past evolution of a region and its climate as well, and provides clues for understanding the origin and geological histories of the region. Continental sediments are especially heterogeneous as a result of the erosion of various continental rocks. After formation, sediments can be tectonically deformed,

redeposited or even subducted and therefore enter the deep Earth cycle (Sobolev et al., 2007; Trubitsyn et al., 2007; Bobrov and Baranov, 2018).

West Antarctica is characterized by weak stretched lithosphere and hot upper mantle with mantle upwelling flow (Danesi and Morelli, 2001; Morelli and Danesi, 2004; Lucas et al., 2020). Stretching began in the Mesozoic (and even earlier) and continues now in some parts of West Antarctica, for example, Terror Rift (Behrendt, 1999; Davey et al., 2006). In West Antarctica, the bottom of the ice sheet in Bentley, Byrd and Ronne depressions (BST, BB, Figure 1) reaches -2000 m and more below sea level (Morlighem et al., 2020). West Antarctica is characterized by large sedimentary basins. The Ross Ice Shelf (Figure 1) is a broad region characterized by low subglacial topography. It is part of the West Antarctic Rift System, formed by stretched continental crust (Ji et al., 2018). The Byrd and Bentley (BB, BST, Figure 1) subglacial basins are a continuation of the Ross Ice Shelf along the Transantarctic Mountains, with very low subglacial topography. Another large sedimentary basin of West Antarctica is under Filchner-Ronne Ice Shelf. It has been suggested that Filchner-Ronne Ice Shelf is a failed Jurasic rift (Jokat and Herter, 2016). Now it is a passive continental margin unlike the West Antarctic Rift System.

East Antarctica, in contrast, is characterized by rather strong and thick lithosphere with mantle downwelling flow under it (Danesi and Morelli, 2001; Morelli and Danesi, 2004; Chuvaev et al., 2020). In the past, however, East Antarctica has also experienced extension during the breakup of Gondwana, suggesting that there are extensive sedimentary basins for East Antarctica as well. Some of the sedimentary basins are isolated inside the continent, while others have access to the shelf and continental sediments, thus being carried out into the surrounding seas. In East Antarctica, the deepest onshore depression, the Denman depression, was recently discovered, with

77 bottom reaching 3500 m below sea level (Morlighem et al., 2020). Other deep
78 depressions have also been found, mainly in the Australo-Antarctica block of East
79 Antarctica. Their relief resembles the East African Rift System; the Vostok, Astrolabe
80 and Adventure depressions are similar to the structures of lakes Tanganyika, Nyasa,
81 and the Baikal Lake in Siberia. Obviously, such deep depressions are a trap for
82 sediments, if they formed before glaciation of the continent.

83 Recently, several regional and global models of sediments have been built. Global
84 compilations of sediment thickness have been published by Laske and Masters (1997);
85 Divins (2003); Laske et al. (2013); Straume et al. (2019), and others. Regional sediment
86 models in the Antarctic region have been compiled by Whittaker et al. (2013) for the
87 Australo-Antarctic region; Huang et al. (2014) for Weddell Sea; Wobbe et al. (2014)
88 and Lindeque et al. (2016) for the West Antarctic margin; Straume et al. (2019) for
89 sediment thickness in the world's oceans (include previous sediment models); Baranov
90 et al. (2021) for the whole Antarctic continent.

91 Thus, for the South region there are two recent sediment models: GlobSed for the
92 South Oceans (Straume et al., 2019) and ANTASed for the Antarctic continent (Baranov
93 et al., 2021). Each of these models has been obtained independently from large
94 amounts of geophysical data. It appears necessary then to combine these two models
95 into a single sediment model for the whole Southern region.

96 The depth to the basement is among the parameters most reliably determined
97 by seismic data. However, geophysical data can also provide information about
98 structure and other properties of sediments, giving hints about their origin. Except for
99 the studies by Bassin et al. (2000); Laske et al. (2013) and Baranov et al. (2018a), no
100 models have been focused on investigating the inner sedimentary structure for the
101 Antarctic region. However, global models CRUST2.0 (Bassin et al., 2000) and CRUST1.0

(Laske et al., 2013) have poor accuracy in Antarctica and do not provide information about data coverage. It is thus unknown where these models are based on real data and what geophysical datasets have been used. Moreover, geophysical data obtained after 2013 have not been incorporated in the compilation of CRUST1.0. We argue that some old seismic profiles have not been included in CRUST1.0 too. The regional sediment model from Baranov et al. (2018a) used seismic data, but not, e.g., the old seismic profiles from Beaudoin et al., 1992, Bentley (1973), McGinnis et al (1985), Ten Brink et al (1993) and others, and did not use other geophysical data (magnetic, radar and new BEDMACHINE subglacial relief). In addition, it does not include part of the sedimentary basins mainly from the Australo-Antarctica block.

Large differences in the thickness and properties of the Antarctic crust between the CRUST1.0 model (Laske et al., 2013) and the improved ANTMoho model (Baranov et al., 2021) suggest the need to revise the properties of the sedimentary model of Antarctica. In this study, we first update a previous model (ANTASed, Baranov et al., 2021) on the basis of geophysical data, not considered before, related to sedimentary basin structure; and then we combine the sediment grid of the new Antarctic continental model (ANTASed-II), together with information about the South Ocean (GlobSed, Straume et al., 2019) into a continuous 5-arc-minute sediment thickness grid,. The differences between total thickness of sediments in CRUST1.0 and in our combined model are also presented. In CRUST1.0, sediments are usually divided into upper, middle and lower layers. We use the same structure for consistency with global CRUST1.0 model. Main parameters of sediment layers are depth, thickness, and P wave velocities. We therefore use seismic data to construct the new three-layer sediment model. The average P-wave velocity diagrams for sedimentary basins in

Antarctica is presented too. The new model is then analyzed and compared to CRUST1.0 sediment model.

2. Methods and data

2.1 Combining ANTASed and GlobSed into a single model

GlobSed (Straume et al., 2019) and ANTASed (Baranov et al., 2021) are natively represented with different projections, that need to be homogenized. GlobSed is presented as a Cartesian 5-arc-minute sediment thickness grid whereas ANTASed is presented as a pole-equidistant grid created with an azimuthal equidistant projection centered at the South Pole. The relationship between the coordinates (ϑ, ρ) of the point on the globe in the azimuthal equidistant projection with the center in the South Pole, and its latitude and longitude coordinates (φ, λ) are given by the equations (Snyder and Voxland, 1989):

$$\rho = (\pi/2 + \lambda) \times \cos(\varphi) \quad (1)$$

$$\theta = (\pi/2 + \lambda) \times \sin(\varphi) \quad (2)$$

At first, we chose to convert the GlobSed dat file to an azimuthal equidistant projection with center in the South Pole— that we deem more appropriate for the high-latitude geographical region.

Then we build a 5-arc-minute grid using a kriging technique for interpolation (linear variogram; SURFER, Golden Software package). This method has been described in detail and used for Moho constructing in different regions (Baranov, 2010; Baranov and Morelli, 2013; Baranov et al., 2018a; Baranov et al., 2018b). We then blank out the resulting grid by the continental shelf border (Fig. 1a) and convert the blanked grid to a data file. We thus obtain the thickness of sediments, in an

appropriate polar projection, for the South Ocean surrounding continental Antarctica. Similarly, to the GloblSed model, we convert the sediment thickness data from the CRUST 1.0 model to azimuthal equidistant projection for further comparison with our combined sediment model and build the 5-arc-minute grid using the same a kriging technique (Fig. 1b).

Further we significantly improve the continental model for some important regions. To construct the new ANTASed-II model, we add fresh information from newly accessed data to previously published model ANTASed (Baranov at al., 2021). Specific references for different regions are mentioned in the following. We start from the contour levels in ANTASed by comparing their values to 2D seismic profile data, and manually update the thickness values preserving the shapes of contours. This is quite a labour-intensive endeavour, but it is necessary to prevent unrealistic features correlated to data distribution along linear profiles. During this procedure, we consider other information — such as the BEDMACHINE bedrock model — as prior geological information. Finally, the model consisting of (updated) contour levels is interpolated to values on regularly-spaced grid points using kriging.

We delineate the contours of the Antarctic Peninsula and Alexander I Island more clearly, obtaining a new sedimentary basin under the George VI Ice Shelf between them. This is confirmed by the BEDMACHINE model and different geophysical data (Bell and King, 1998, Crabtree et al., 1985; Maslanyi, 1988). In the central part of Ross Ice Shelf sediment thickness is rather moderate (1-2 km) as confirmed by seismic profiles UPC, SERIS, CIR and UPB (Rooney et al., 1987; Munson and Bentley, 1992; ten Brink et al., 1993). In the Byrd and Bentley basins sediments are about 2-4 km thick, according to seismic profiles BB`, CC` (Bentley, 1973), and in

175 the area around McMurdo Sound sediments reach up to 4 km and more (Beaudoin et
176 al., 1992; ten Brink et al., 1993).
177 For East Antarctica we add new Frost and Sabrina subglacial basins in the
178 Australo-Antarctica block. These basins are added according to a more thorough
179 analysis of various geophysical data: magnetic data from Aitken et al (2014); subglacial
180 relief from BEDMACHINE model (Morlighem et al., 2020); paleotopography
181 reconstructions (Wilson and Luyenduk, 2009); and gravity anomalies (Sheinert et al.,
182 2016). We also use these data to more accurately map existing sedimentary basins:
183 Wilkes, Aurora, Astrolabe, Adventure, and others. We also use old seismic data for
184 improving Lambert basin borders (Fedorov et al., 1982; Kurinin and Grikurov, 1982).
185 Two seismic profiles cross Lambert graben. The first profile AB, lying approximately at
186 70^0 S, provides 6-9 km of multilayer sediments under Amery Ice Shelf between Prince
187 Charles Mountains and Larsemann Hills as a single sedimentary basin. At the same
188 time, the lower layer with 1-2 km thickness consists of high-velocity Permian
189 sediments, and Cenozoic sediments lie on the top. For this profile, the northern
190 extension of the Mawson Escarpment does not come to the surface and is covered
191 with sediments with 1–2 km thickness but is clearly visible below. To the south, on the
192 second profile AA` (Prince Charlez Mountains, Lambert Rift, Grove Mountains), a single
193 basin is divided into two branches, delineate two sediment basins, which are
194 separated by the Mawson Escarpment in the middle. At the same time, the thickness
195 of sediments in the eastern branch between the Mawson Escarpment and the Grove
196 Mountains is even higher (up to 6 km) than in the western branch between the Prince
197 Charlez Mountains and the Mawson Escarpment. However, the eastern part in the
198 surface subglacial relief is weakly expressed in contrast to the western part. In the

199 eastern branch of the Lambert Basin, there is another escarp of basement rocks that
200 does not come to the surface.
201 After adding new geophysical data we rebuild the improved ANTASed model to
202 5-arc-minute grid in spherical azimuthal equidistant projection for compatibility with
203 CRUST 1.0 and GlobSed grids, blank the ANTASed-IIgrid by the continent margin (Fig.
204 1c) and convert the blanked grid to a data file. Next, we merge together the revised
205 ANTASed, and the GlobSed data files. Using the kriging interpolation method with
206 linear variogram (Golden Software package) we finally interpolate the resulting data
207 array onto a geographical grid created with an azimuthal equidistant projection
208 centered at the South Pole. The kriging parameters were chosen as follows: the
209 interpolation area was from the South Pole to 60°S, the 5-arc-minute grid step on a
210 geographical latitude-longitude grid with no anisotropy, and the scale was set one.
211 This technique can be used to combine heterogeneous data files into a single one.
212 To find the difference between the new ANTASed-II model and the previous
213 ANTASed sediment model, and between the new combined sediment model for
214 Antarctica and surroundings and the CRUST1.0 sediment model, we subtract the 5-arc-
215 minute ANTASed sediment grid (CRUST 1.0 sediment grid) in spherical azimuthal
216 equidistant projection from the new received model grids (ANTASed-II and combined)
217 in the same projection respectively using grid manipulation modules of the Generic
218 Mapping Tools (Wessel et al., 2019).
219

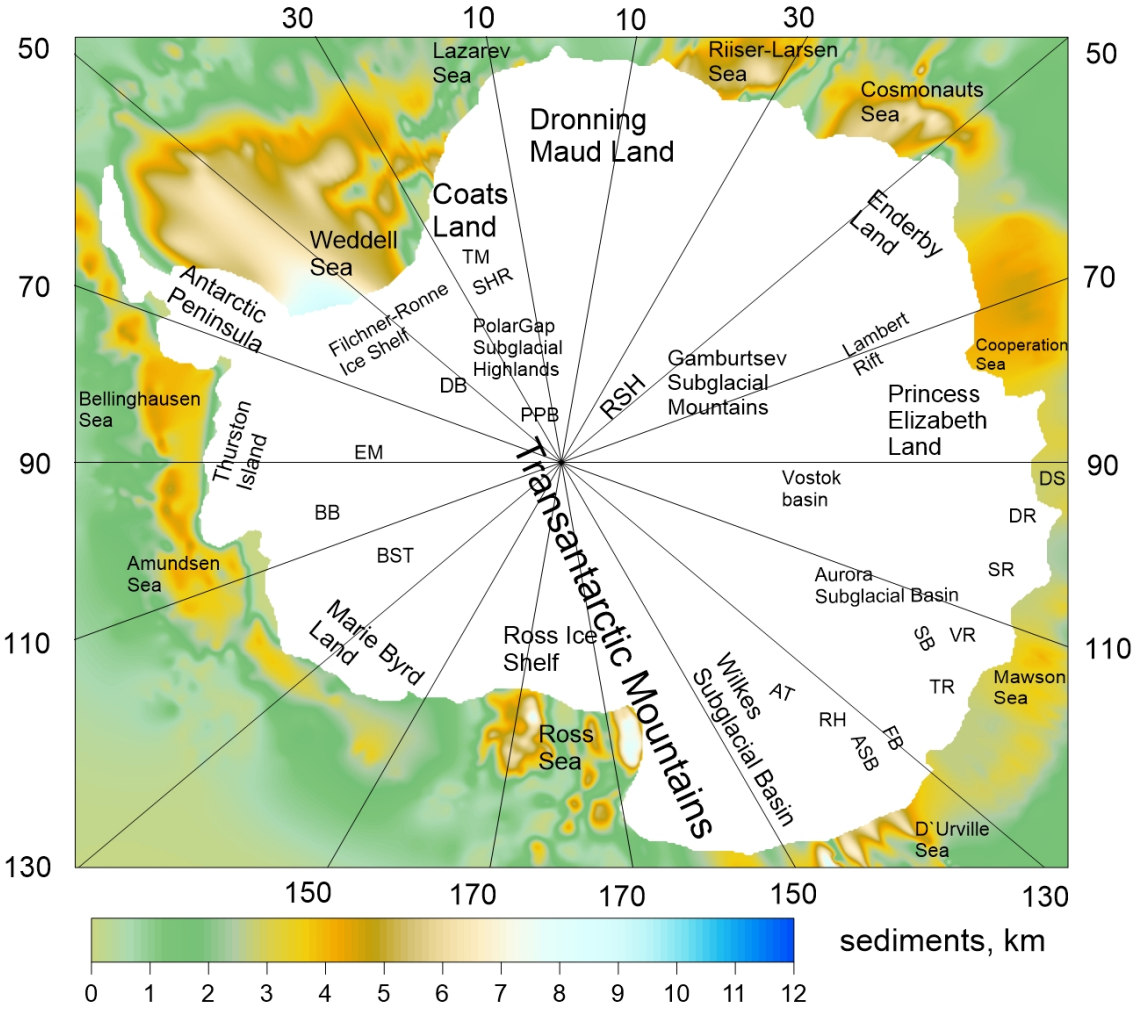

220

221 **Fig.1a.** Map of the sediment thickness from GlobSed (Straume et al., 2019) in the

222 azimuthal equidistant projection. Used abbreviations: PPB - Pensacola-Pole Basin, EM -

223 Ellsworth Mountains, BB – Byrd Basin, BST – Bentley Subglacial Trench, SHR-

224 Shackleton Range, TM - Theron Mountains, SR - Scott rift, DR - Denman rift, VR -

225 Vanderford rift, TR - Totten rift, AT - Adventure Trench, ASB - Astrolabe Subglacial

226 Basin, RH - Resolution Highlands, DB - Dufek Block, RSH - Recovery Subglacial

227 Highlands, FB – Frost Subglacial Basin, SB – Sabrina Subglacial Basin, DS – Davis Sea.

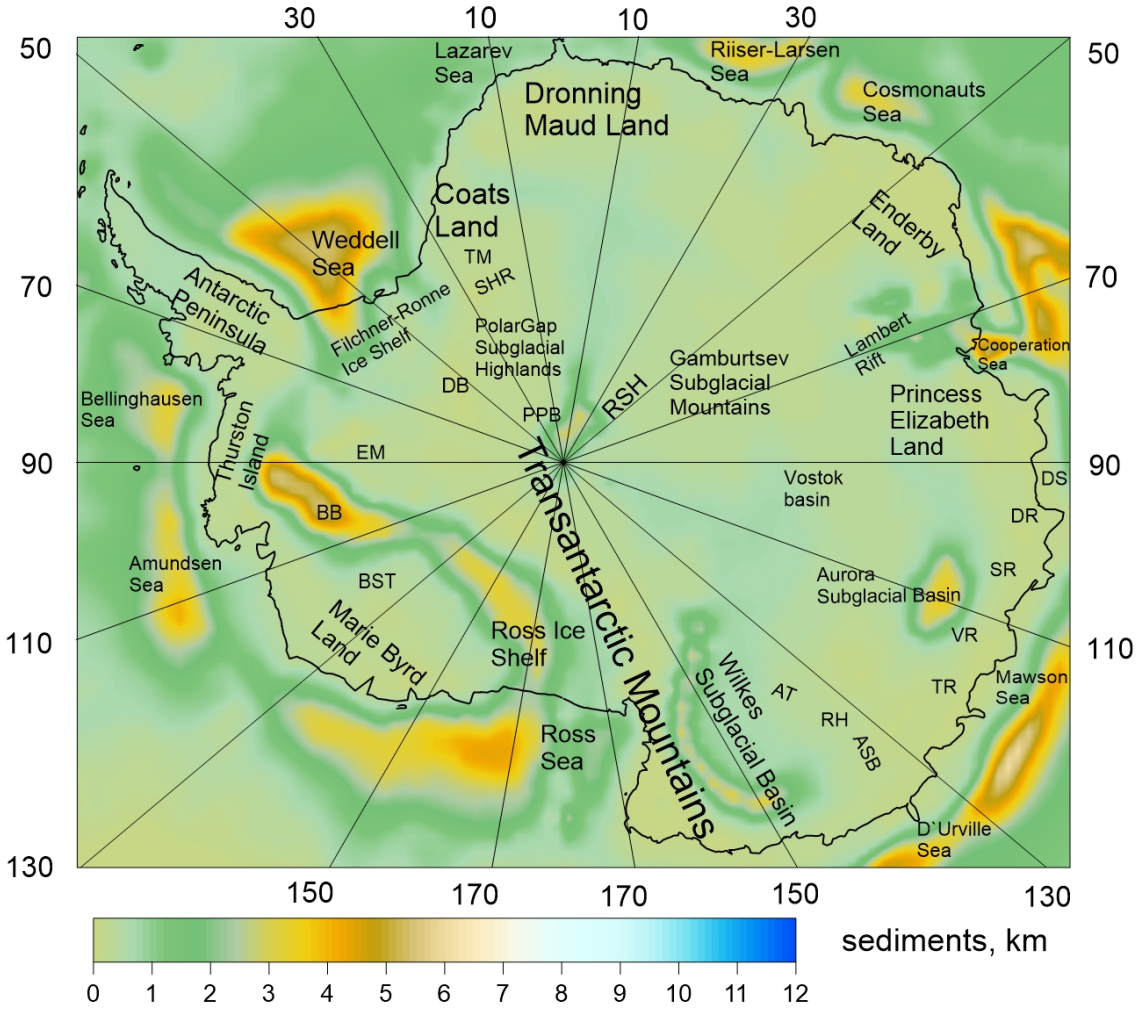

228

229 **Fig.1b**. Map of the sediment thickness from CRUST 1.0 model (Laske et al., 2013). The

230 same abbreviations as in Fig.1a are used.

231

232

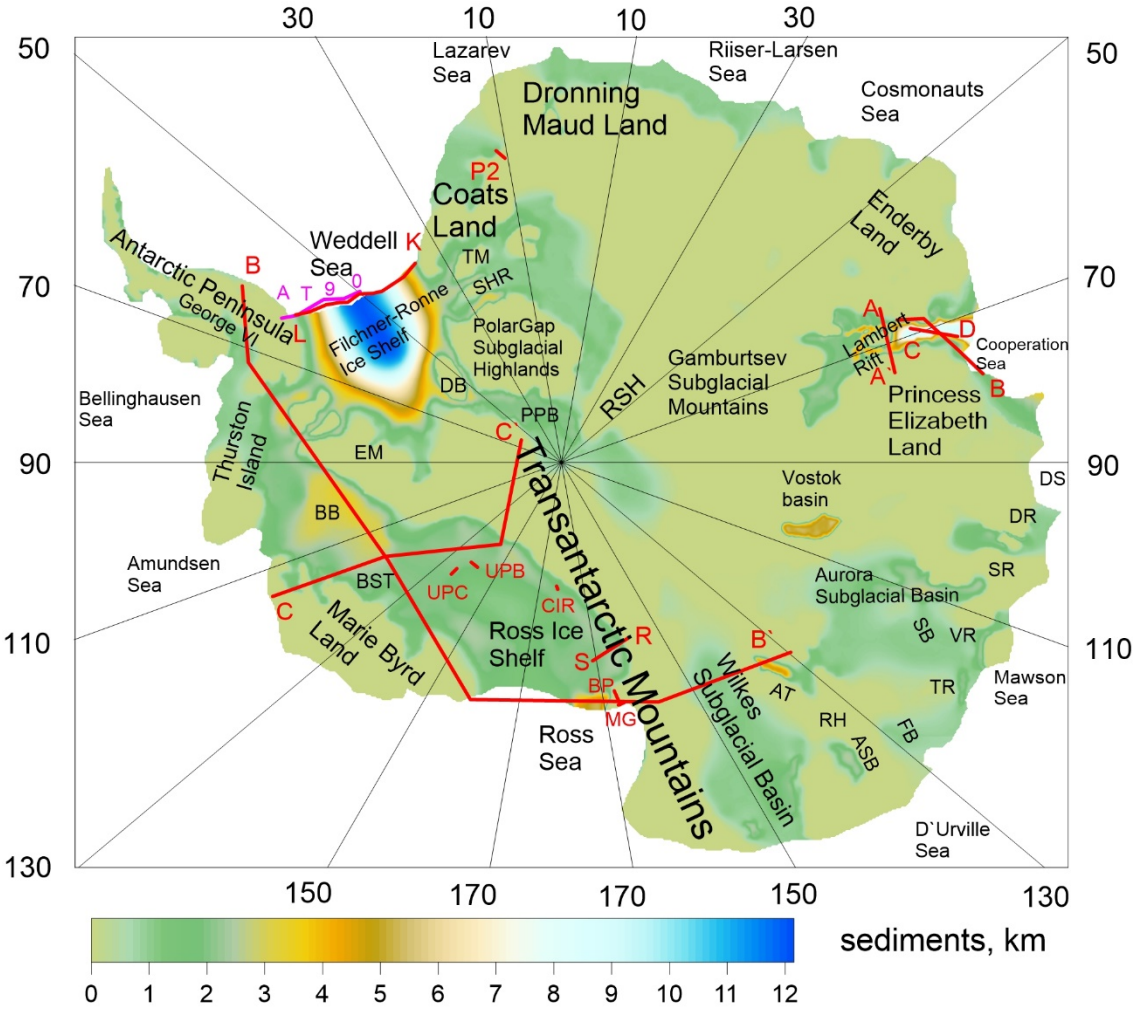

Fig.1c. Map of the sediment thickness from our new ANTASed-II sediment model (this study). The same abbreviations as in Fig.1a are used. Seismic profiles containing information about sediment velocities are shown as red lines: BB`, CC` (Bentley 1973); LK (Leitchenkov and Kudryavtzev, 1997); P2 (Hungeling and Tyssen, 1991); AB, CD, AA` (Kolmakov et al., 1975; Fedorov et al., 1982); MG (McGinnis et al., 1985); BP profile (Beaudoin et al., 1992); SR (Ten Brink et al., 1993); CIR, UPB (Rooney et al., 1987); UPC (Munson and Bentley, 1992); ANT II/4, 90200, 92010 profiles (Hübscher et al., 1996) are shown by magenta lines (symbols A, T, 9, 0). The interpretation of the profiles is also given in Table 1.

2.2 Three-layer sediment model

245 The depth to the basement is among the parameters most reliably determined
246 from seismic data, and is the main parameter represented by the two input models.
247 Additionally, we also compile elastic properties (P-wave velocity and density). Since
248 these parameters usually increase rapidly with depth, it is necessary to divide the
249 sediment layer into a number, most often three, layers. We hence provide three layers
250 of sediments to ensure consistency with CRUST1.0 (Laske et al., 2013). The first
251 (upper) layer includes sediments with thickness less than 2 km. The middle layer
252 describes sediments below 2 km, whereas the lower layer of sediments lies below 7
253 km. Using this arrangement, we divide the sediment thickness into 3 layers using the
254 merged model for Antarctica region (GlobSed + ANTASed-II database) as a basis. We
255 create separate grids for the upper, middle and lower sedimentary layers using a
256 standard kriging technique with a linear variogram (SURFER, Golden Software
257 package). The kriging parameters are chosen as follows: the interpolation area was
258 from the South Pole to 60°S (on an azimuthal equidistant projection), the 5-arc-minute
259 grid on a geographical latitude-longitude grid with no anisotropy.
260
261 **2.3 Sediment velocity model**
262 Seismic velocity information for sedimentary basins can be provided by
263 different types of seismic data, notably seismic profiles (Deep Seismic Sounding, wide-
264 angle reflection, and refraction profiles). The seismic data used for the analysis of
265 sediment structure are summarized in Table 1. Here we put only intracontinental
266 seismic profiles containing information about inner sediment structure. For the
267 surrounding seas there are also many seismic profiles, but we neglect them as they do
268 not reach on the continent, that is our interest. Obviously, the reliability of this
269 information decreases with increasing distance away from seismic profiles. However,

many sedimentary basins are not large, so one profile alone — combined with information about the shape of the basin — carries significant information. We must also acknowledge that, for a part of sedimentary basins — mainly from the Australo-Antarctica block — there are no any seismic data at all.

Source	Type	Sediment properties	Region	Additionally,
Bentley, 1973	Long seismic refraction profiles	Ross Ice Shelf (2.4 km/s for upper sediments, 4.2 km/s for middle sediments) - BB' profile Byrd and Bentley sedimentary basins (4.1 and 4.3 km/s for upper sediments) - BB' profile Bentley basin (4.3 km/s for upper sediments) - CC' profile	BB' profile: Antarctic Peninsula – Victoria Land; CC' profile: Marie Byrd Land–Transantarctic Mountains	These profiles provide information for sediments and upper crust
Hungeling and Tyssen, 1991	Refraction profile	4.7 km/s for sediments	P2 profile: Western Dronning Maud Land near the coast	This profile provides information for sediments and crust
Fedorov et al., 1982; Kurinin and Grikurov, 1982; Kolmakov et al., 1975	Three DSS profiles	Upper layer of sediments 2.0-3.0 km/s; middle layer 3.5-3.7 km/s lower layer 4.0-4.5 km/s	AB profile: Prince Charles Mountains, Lambert Rift, Princess Elizabeth Land; AA` profile: Prince Charles Mountains, Lambert Rift, Mawson Escarpment, Lambert Rift, Grove Mountains; CD profile: Lambert Rift	These profiles provide information for sediments and crust
McGinnis et al., 1985	Refraction profile	2.5 km/s s for upper sediments	MG profile: Near Ross Island	This profile provides information for sediments and crust
Rooney et al., 1987	CIR and UPB refraction profiles	CIR profile: 4.0 km/s for upper sediments; UPB profile: 2.0 km/s for upper sediments	CIR profile is located in Ross Ice Shelf near Shackleton Glacier; UPB profile is located near the Siple Coast, West Antarctica	Only sediments and upper crust

Munson and Bentley, 1992	Refraction, wide-angle reflection UPC profile	2.0 km/s for upper sediments	UPC profile: West Antarctica between Bentley Subglacial Trench and Siple Coast	Only sediments and upper crust
Ten Brink et al., 1993	Refraction, wide-angle reflection SERIS profile	2.2-2.6km/s for upper sediments	SR profile: border between Ross Ice shelf and Transantarctic Mountains (near Nimrode Glacier)	This profile provides information for sediments and crust
Beaudoin et al., 1992	Refraction and reflection profiles	2.7 km/s for upper sediments; 4.2 km/s for lower sediments	BP profile: near Ross Island, the profiles are aligned approximately perpendicular to the Cenozoic alkaline volcanics of the Ross Archipelago	Only sediments and upper crust
Hübscher et al., 1996	Two refraction and one reflection profiles	Upper layer of sediments (with ice and water) 2.2 km/s; middle layer 3.5 -3.7 km/s; lower layer 4.1-4.8 km/s	ANT II/4, 90200, 92010 profiles: Ronne Ice Shelf along the border between Antarctic Peninsula and Berkner Island	These profiles provide information for sediments and crust
Leitchenkov and Kudryavtzev, 2000	DSS profile	Upper layer of sediments 2.6-3.0 km/s; middle layer 3.3-4.0 km/s; lower layer 4.6-4.9 km/s	LK profile: Filchner- Ronne Ice Shelf along the border between Antarctic Peninsula and East Antarctica	Long profile across the main tectonic structures of the Weddell Sea border. This profile provides information for sediments and crust

Table 1. Seismic profiles and origin of sedimentary basins.

For Dronning Maud Land, seismic profile P2 from Hungeling and Tyssen (1991) provides P-wave velocity of about 4.7 km/s for sediments. Seismic data for Lambert Rift provide P-wave velocity in three-layer sediments: upper layer of sediments (2.0-3.0 km/s); middle layer (3.5-3.7 km/s); lower layer (4.0-4.5 km/s) (Fedorov et al., 1982; Kurinin and Grikurov, 1982; Kolmakov et al., 1975). The seismic profile for the Vostok Basin only provides thickness of sediments (Isanina et al., 2009). Similarly, the receiver

283 functions data show the presence of sediments for the Wilkes Basin (Agostinetti et al.,
284 2005). Unfortunately, there are no seismic data on their internal structure for the
285 remaining sedimentary basins of East Antarctica.

286 Some P-wave velocity models from seismic profiles (McGinnis et al., 1985;
287 Rooney et al. 1987; Beaudoin et al., 1992; Munson and Bentley, 1992; ten Brink et al.,
288 1993) provide information about sediment properties for the Ross Ice Shelf. For this
289 region, the P-wave velocity varies from 2.0 to 4.2 km/s. Several refraction profiles near
290 Ross Island provide information about crustal and sedimentary properties (McGinnis
291 et al., 1985). Here the P-wave velocity in the sedimentary layer is about 2.5 km/s.
292 Refraction profile CIR reveals one sediment layer with P-wave velocity of about 2.4
293 km/s for the Ross Ice Shelf near Transantarctic Mountains (Shackleton Glacier).
294 Another refraction profile (UPB) reveals one sediment layer (4.0 km/s) near the Siple
295 Coast (Rooney et al., 1987). The refraction and wide-angle reflection profile UPC
296 between Bentley Subglacial Trench and Siple Coast provide P-wave velocity of about
297 2.0 km/s for upper sediments (Munson and Bentley, 1992). Refraction and reflection
298 profiles lying perpendicular to the Cenozoic alkaline volcanics of the Ross Iceland
299 reveal a P-wave velocity in sediments of about 2.7 km/s and 4.2 km/s for upper and
300 middle sedimentary layer respectively (Beaudoin et al., 1992). At the border between
301 Transantarctic Mountains and Ross Ice Shelf, near the Nimrode Glacier area, seismic
302 profile SERIS reveals P-wave velocity in sediments of about 2.2-2.6 km/s (Ten Brink et
303 al., 1993).

304 Under the Filchner-Ronne Ice Shelf, a large subglacial basin lies between the
305 Antarctic Peninsula and East Antarctica. This basin is characterized by low bedrock
306 topography. A 800 km-long DSS profile has been carried out across the Filchner- Ronne
307 Ice Shelf (Leitchenkov and Kudryavtzev, 2000). This profile reveals a complex

multilayer sedimentary basin and provides quite detailed data about sediment structure of this region. Sedimentary properties change along the DSS profile near the coastline. The following structure of sediments has been identified: upper layer of sediments with P velocity of about 2.6-3.0 km/s; middle layer (3.3-4.0 km/s) and lower layer (4.6-4.9 km/s). Two refraction profiles between the Antarctic Peninsula and Berkner Island also reveal a complex structure of sediments: an upper layer with P velocity about 2.2 km/s; a middle layer (3.5 -3.7 km/s); and a lower layer (4.1-4.8 km/s) (Hübscher et al., 1996). However, it should be noted that in this study, water and ice have been included in the upper layer of sediments - hence such low velocities in the upper layer. Long seismic profiles AA', BB' and CC' (Bentley, 1973) also provide information about the subglacial structure of Antarctica. Profile AA' does not show a significant amount of sediments. BB' provides velocity for the Byrd and Bentley sedimentary basins (4.1-4.3 km/s) and the Ross Ice Shelf (two layers with 2.4 and 4.2 km/s respectively). The third seismic profile CC' provides 4.3 km/s for the Bentley sedimentary basin.

It is indeed quite difficult to estimate uncertainties of a three-layer model that has been obtained by merging different types of data with large empty gaps. Unfortunately, for many areas we had only one data source, so we had no possibility to evaluate uncertainties. The accuracy of the seismic profiles seems however to be quite high. The best resolution for seismic boundaries in crust and sediments is often obtained using reflection profiles. Intermediate resolution can be obtained using refracted and wide-angle reflected waves. The accuracy for these methods is of the order of 1–2 km (Kanao et al., 2011). However, due to the vastness of sedimentary basins, the parameters of sediments far from the profiles can differ significantly.

3. Results

3.1 Combined sediment model

The combined sediment thickness for Antarctica and surroundings, derived from merging our improved continental sedimentary model ANTASed-II with the Southern Ocean model GlobSed from Straume et al. (2019), is shown in Fig. 2a.

The marginal seas of Antarctica contain a significant amount of sediments (with 2-6 km thickness). The thickest sedimentary basin is located under the Filchner Ronne Ice Shelf (up to 12 km, with multilayer sediments). At the same time, towards the Weddell Sea, the thickness of sediments decreases to 6-8 km. Another large sedimentary basin lies under the Ross Ice Shelf and Ross Sea (1-6 km) with a continuation to Byrd and Bentley basins. In the southern part of the Ross Sea, the sedimentary basins of Victoria Land, the Central and Eastern sedimentary basins (between which lie the Coulman High and Central High seamounts) are distinguished. Bentley and Byrd basins have 2-3 km of sediments. New revealed George VI basin has 1-2 km of sediments.

Sedimentary basins of East Antarctica are less extensive but also diverse. Pensacola-Pole and South Pole basins have about 1-2 km of sediments. The narrow and deep Coats Land depressions are extensions of the Filchner-Ronne basin (1-3 km of sediments). In the western part of Dronning Maud Land near the coast we find sedimentary basins 1-2 km thick, and the deep younger sediment-filled JutulStraumen Rift between the western and eastern parts of Dronning Maud Land. In the eastern part of Dronning Maud Land, near the coast, there are sedimentary basins too (1-2 km). Between Enderby Land and Princess Elizabeth Land, the deep Lambert Rift lies with continuation to the Cooperation Sea. It is characterized by multilayer sediments

with thickness up to 8 km or more, formed during the breakup of Gondwana and possibly earlier (Boger and Wilson, 2003; Lisker et al., 2003; Whitehead et al., 2006).

East of the coast, two narrower and deep rifts begin: Scott and Denman. There are no seismic data for them. Geophysical data and analogy with other Antarctic rifts indicate sediments with thickness about 1-2 km. The vast inland Vostok sedimentary basin lies to the southeast. Here seismic data show multilayer sediments with thickness of up to 5 km. The elongated Aurora basin, lying in the intercontinental realm of the Australo-Antarctica block, has 1-3 km of sediments. The recently discovered Vanderford and Totten rifts are characterized by sediments with thickness up to 2 km. Newly revealed Frost and Sabrina sedimentary basins have 1-2 km of sediments. Two other intracontinental basins in the Australo-Antarctica block (Adventure and Astrolabe) have 2-4 km of sediments. In these basins, seismic data are absent. Finally, the Wilkes basin has sediments about 1-3 km thick.

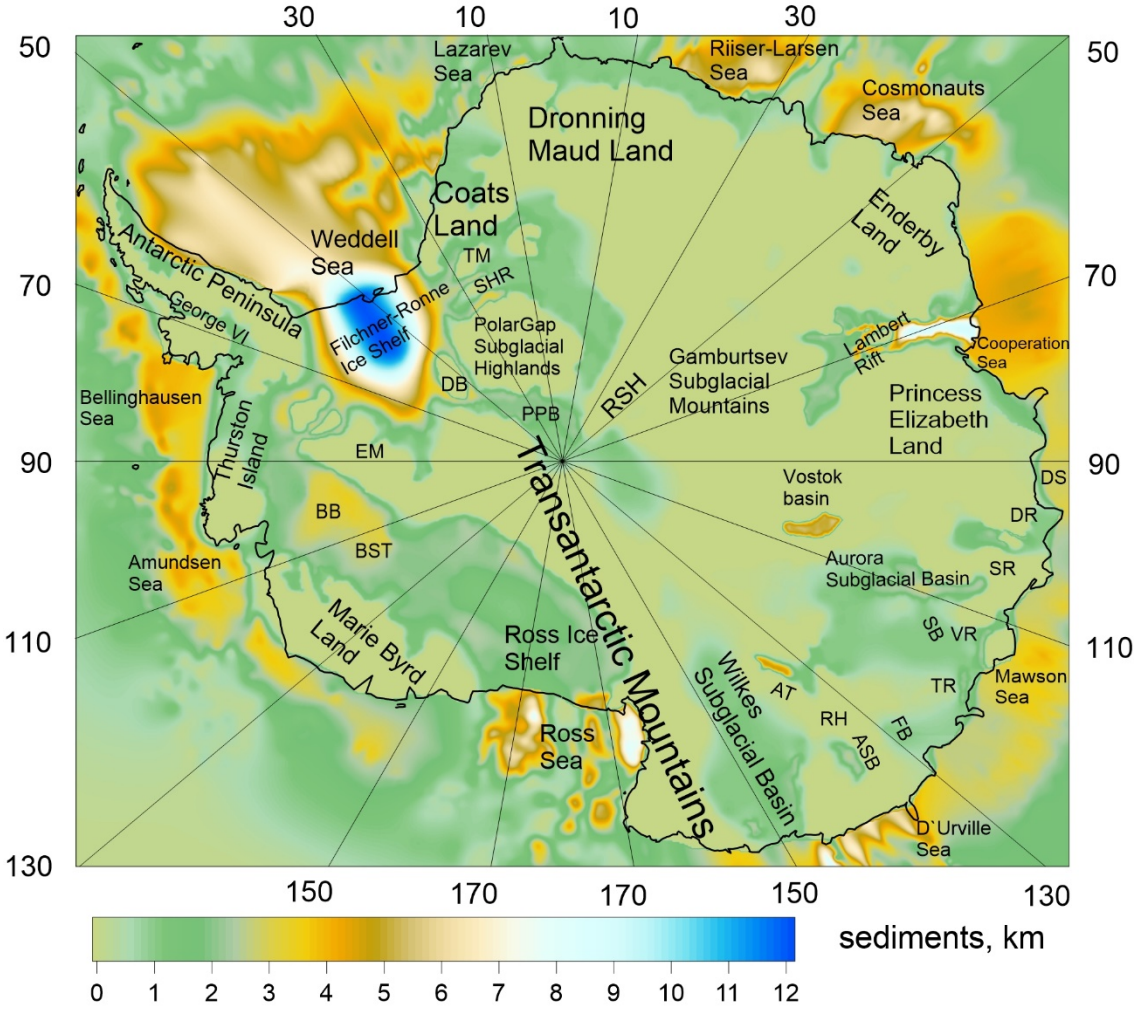

Fig. 2a. Combined map of a sediment thickness for Antarctica (improved ANTASed-II model, (Baranov et al., 2021)) and surroundings (GlobalSed model, Straume et al., 2019). It is used the same abbreviations as in Fig.1a.

The difference between our new ANTASed-II sediment model (this study) and and the previous ANTASed model (Baranov et al., 2021) is −6/+5 km (mean -0.1 km, standard deviation 0.73 km, see Figure 2b). There are significant differences in regions such as under the Filchner-Ronne Ice Shelf (-6 km), basins of Coats Land (−1 km), coastal basins of Dronning Maud Land (about 1 km), Lambert Rift and surroundings (-5 / +5 km), Denman, Scott, Vanderford and Totten rifts (-2 / +1 km), Vostok Basin (-2

383 km), Aurora Basin (-3/+1 km), Sabrina Basin (+1 km), Frost Basin (+1 km), Adventure
384 Basin (1–2 km), Astrolabe Basin (about 1 km), Wilkes Basin (-1/+1 km), Ross Ice Shelf (-
385 3 km), Bentley and Byrd basins (−2 km), South Pole Basin (about 1 km), Thurston Island
386 (about 1 km), Antarctic Peninsula (about 1 km).

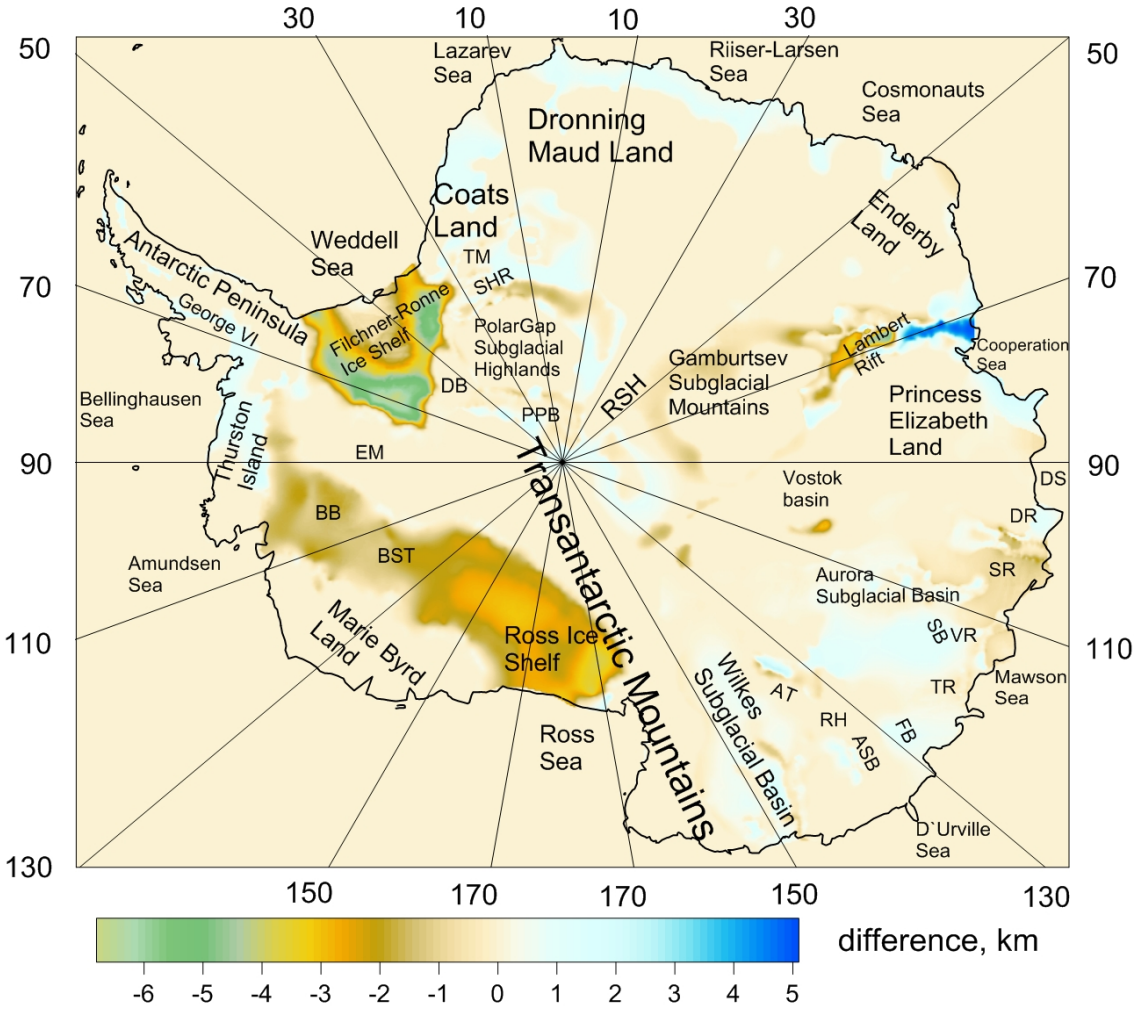

387

388 **Fig. 2b.** Difference between new ANTASed-II sediment model (this study) and the
389 previous ANTASed model (Baranov et al., 2021). It is used the same abbreviations as in
390 Fig.1.

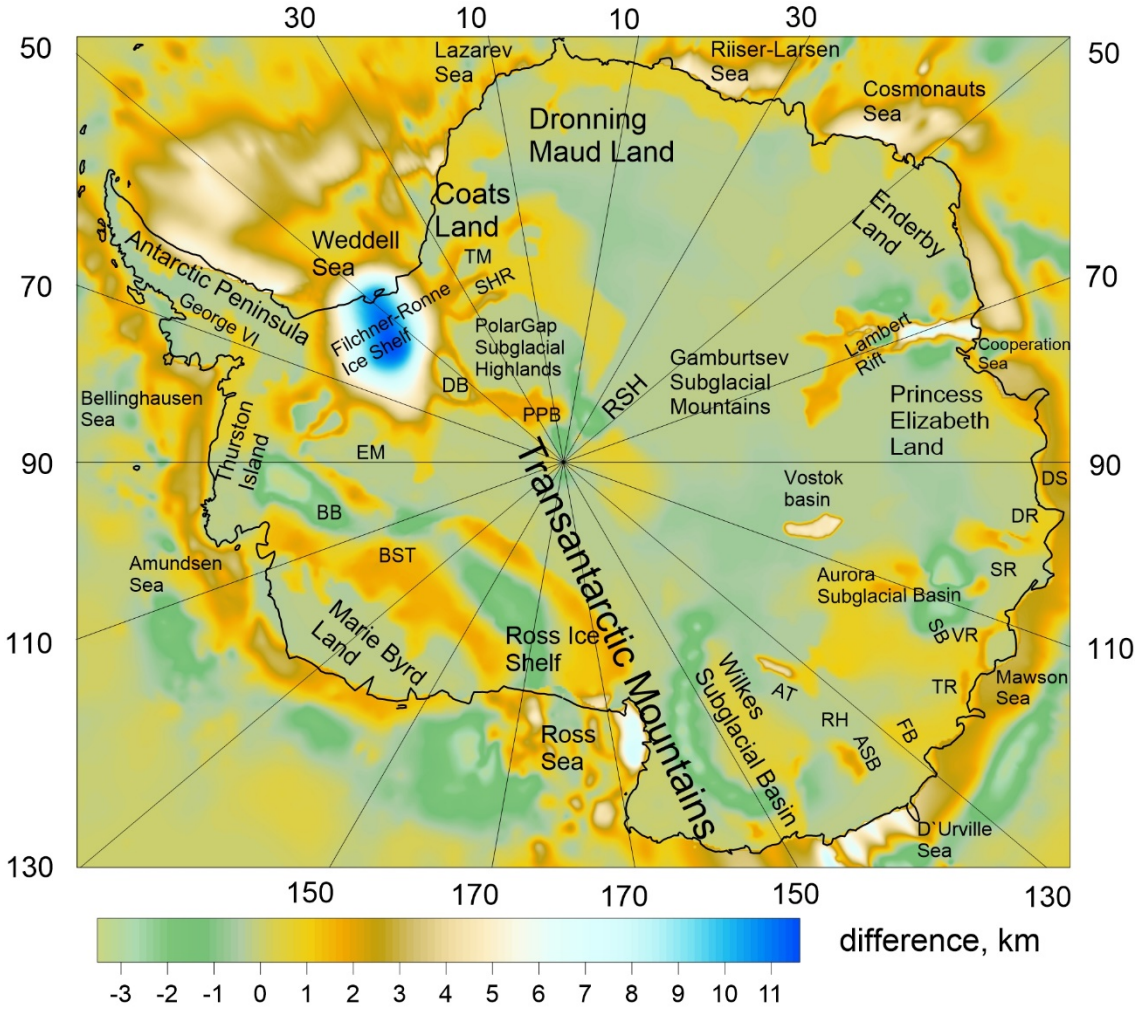

Fig. 2c. Difference between merged sediment model (GlobSed and ANTASed-II) and the CRUST1.0 model. It is used the same abbreviations as in Fig.1.

The difference between our combined sediment model (this study) and CRUST 1.0 (Laske et al., 2013) is −3/+11 km (mean 0.52 km, standard deviation 1.56 km, see Figure 2c). There are significant differences in regions such as under the Filchner-Ronne Ice Shelf (+11 km), Weddell Sea (+5 km), basins of Coats Land (−2/+3 km), coastal basins of Dronning Maud Land (about 1 km), Lazarev Sea (+1/+2 km), Riiser-Larsen Sea (1-2 km), Cosmonauts Sea (-1/+4 km), Lambert Rift and surroundings (-2 / +7 km), Cooperation Sea (-1/+4 km), Denman, Scott, Vanderford and Totten rifts (1-2 km), Vostok Basin (3-5 km), Davis Sea (1-2 km), Aurora Basin (-3/+1 km), Sabrina Basin (+1 km), Frost Basin (+1 km), Mawson Sea (-3/+2 km), Adventure Basin (2–3 km), Astrolabe Basin (1-2 km), Wilkes Basin (-3/+1 km), D'Urville Sea (-2/+5 km), Ross Ice

Shelf (-2/+5 km), Ross Sea (-3/+7 km), Bentley and Byrd basins (−3/+2 km), Amundsen Sea (-2/+2 km), Pensacola-Pole Basin (1-2 km), South Pole Basin (-2/+1 km), Thurston Island (1-2 km), Bellingshausen Sea (-1/+3 km), Antarctic Peninsula (1-2 km).

3.2 Three-layer sediment structure

We divided sediments into three layers for compatibility with previous global sediment models CRUST 2.0 and CRUST 1.0. We have identified 3 layers in sedimentary basins as described in the Methods section. Upper, middle and lower sediment layers are shown in Fig. 3.

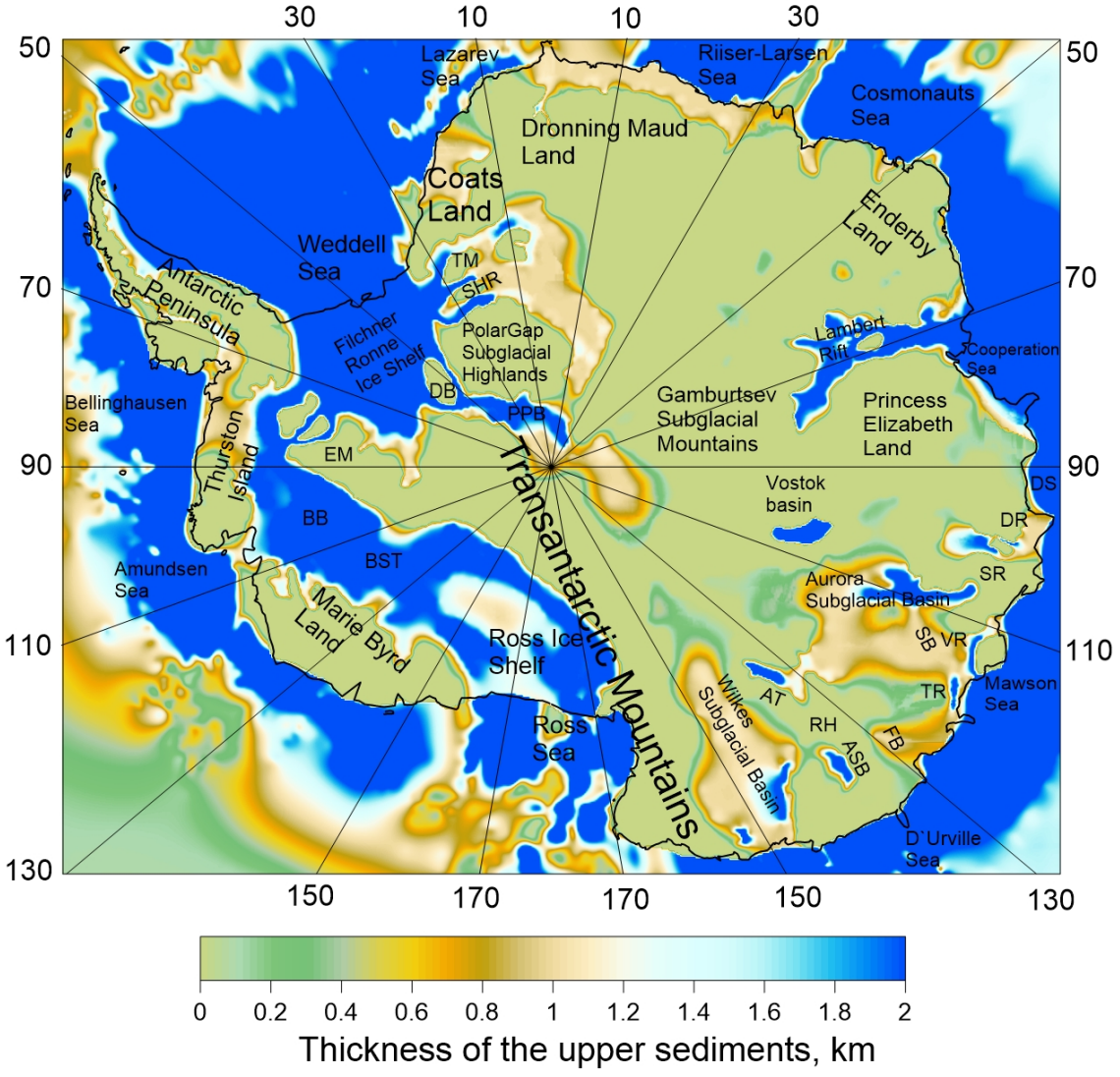

Fig. 3a. Thickness of an upper layer of sediments. It is used the same abbreviations as in Fig.1a.

Figure 3a shows the top layer of sediments (thickness up to 2 km). All sedimentary basins have this layer. West Antarctica is actually a single sedimentary basin and consists of two blocks: the vast Filchner-Ronne Ice Shelf basin with continuation to Weddell Sea, South Pole area and Coats Land; and the vast Ross basin, with continuation to Ross Sea, Bentley trench and Byrd Basin. These two large sedimentary blocks are connected by a deep depression between the Antarctic Peninsula and Ellsworth-Whitmore Mountains and are separated from the marine sedimentary basins on the Pacific Ocean side by the uplifted area of Marie Byrd Land. The sedimentary basins of East Antarctica are less extensive and are not interconnected as in West Antarctica.

There are sedimentary basins in Eastern Antarctica extending into the ocean such as: Dronning Maud Land basins and JutulStraumen Rift with continuation to Lasarev Sea; Lambert Rift with continuation to Cooperation Sea; Scott and Denman rifts with continuation to Davis Sea; Vanderford and Totten rifts with continuation to Mawson Sea; Wilkes basin with continuation to D`Urville Sea. South Pole and Pensacola Pole sedimentary basins have continuation to Filchner-Ronne basin in West Antarctica. Aurora and Sabrina sedimentary basins have continuation to Vanderford and Totten rifts whereas Frost Basin continues to D`Urville Sea. The rest of the East Antarctica sedimentary basins are isolated areas within the Australo-Antarctica block of East Antarctica: Vostok, Adventure and Astrolabe sedimentary basins.

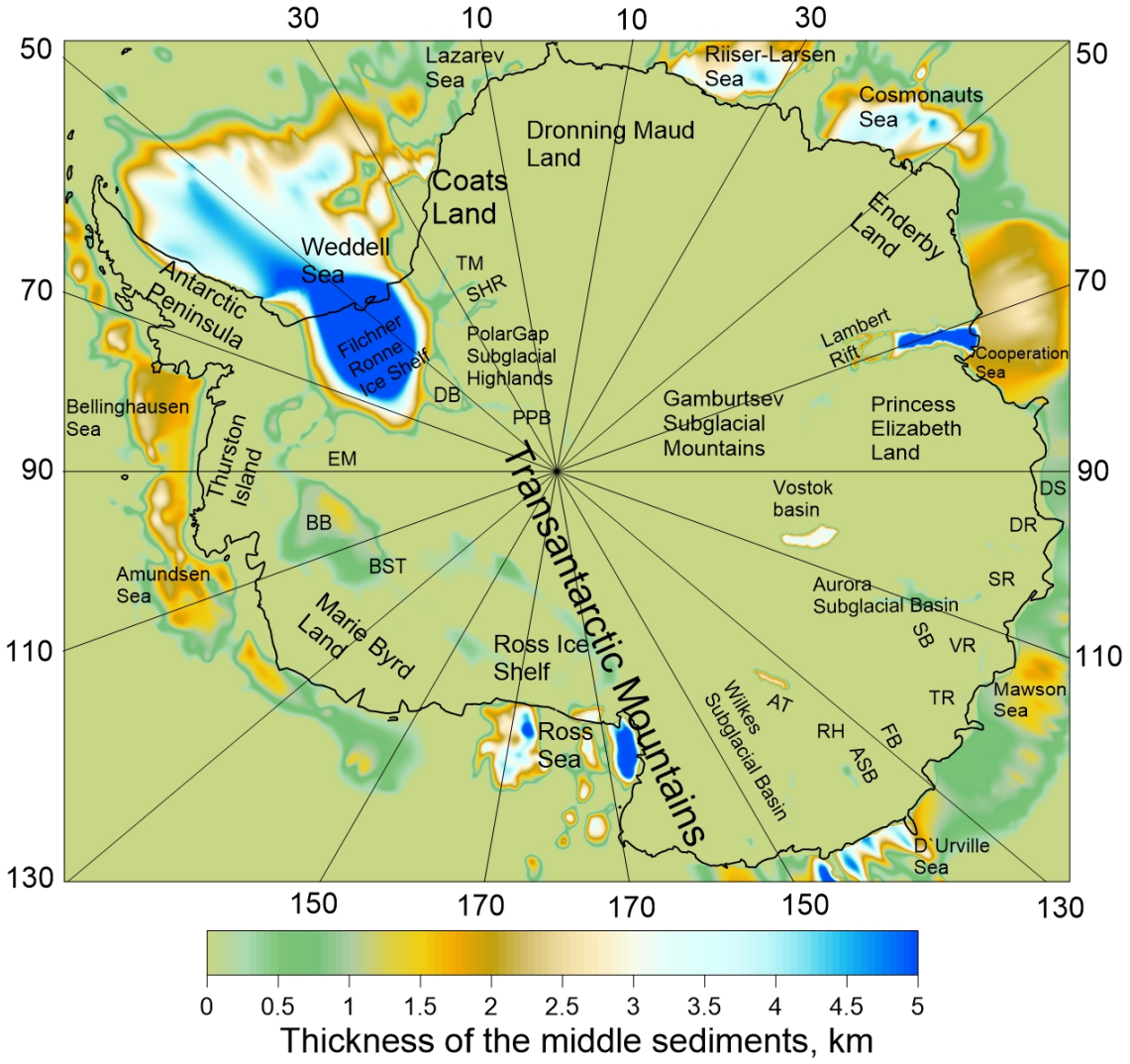

441

442 **Fig. 3b.** Thickness of a middle layer of sediments. It is used the same abbreviations as

443 in Fig.1a.

444

445 As seen in Fig. 3b, a middle layer of sediments (from 2 to 7 km) is present in

446 many basins in Antarctica. In West Antarctica these are Filchner-Ronne Basin (0-5 km),

447 Bentley and Byrd basins (0-2 km), and parts of Ross Ice Shelf Basin (up to 3 km). In East

448 Antarctica the Dronning Maud Land, JutulStraumen, Scott, Denman, Vanderford,

449 Totten, Frost, Sabrina, South-Pole and Pensacola-Pole sedimentary basins do not have

450 a middle layer of sediments. For other sedimentary basins of East Antarctica this layer

451 is present: Coats Land basins (0-1 km), Lambert Rift (0-5 km), Wilkes basin (0-1 km);

Vostok basin (2-4 km); Aurora basin (0-1 km); Adventure and Astrolabe basins (0-2 km).

Significant differences are already visible for this sediment layer in the seas surrounding Antarctica. The most powerful is the continuation of the vast Filchner-Ronne Basin into Weddell Sea (1-5 km). Fragmentally separate deep basins, this layer is present for Ross Sea (0-5 km), Riiser-Larsen Sea (0-5 km), Cosmonauts Sea (0-5 km) and D` Urville Sea (0-5 km). For other marginal seas middle layer has more moderate thickness.

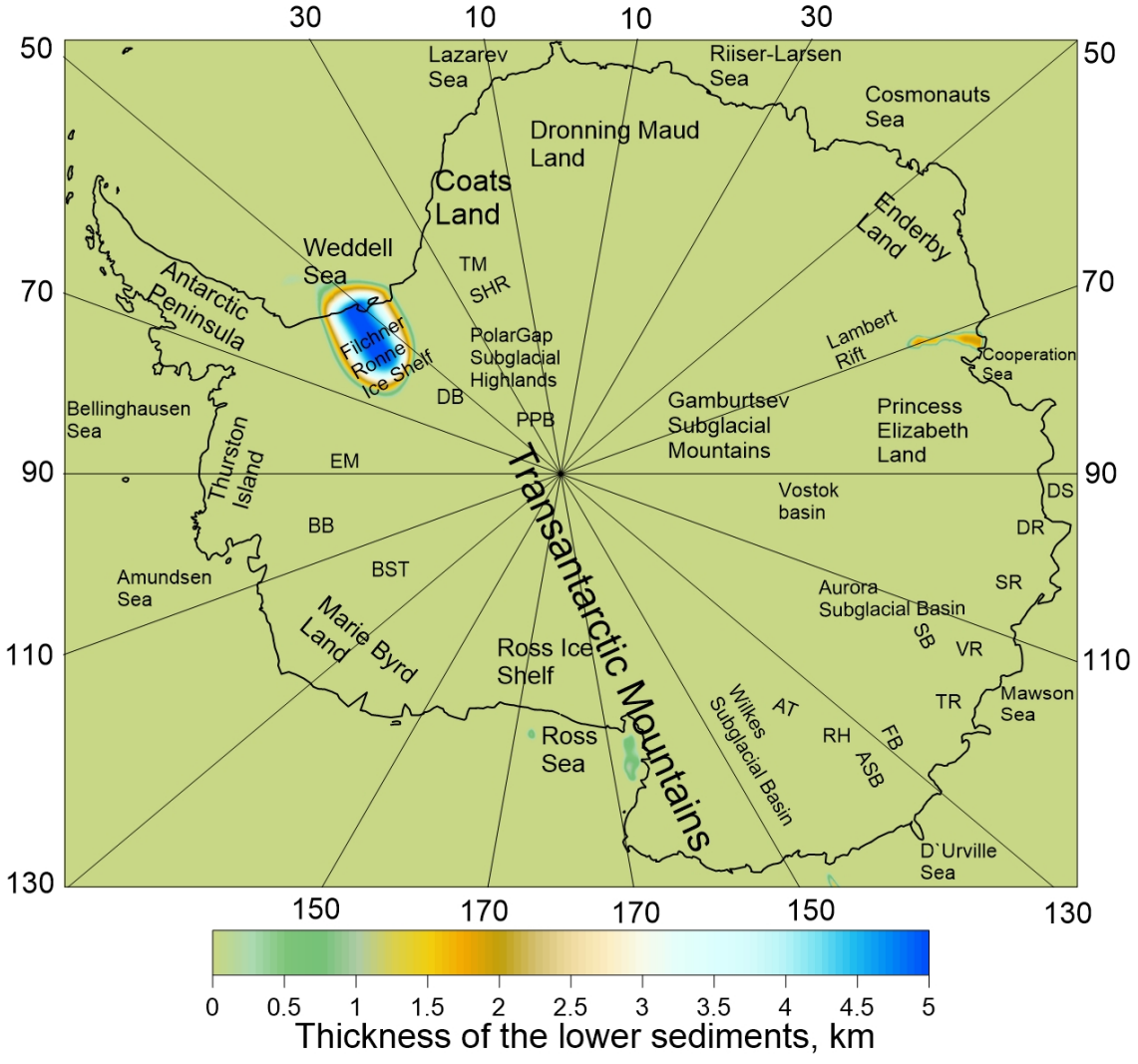

Fig. 3c. Thickness of a lower layer of sediments. It is used the same abbreviations as in Fig.1a.

According to available geophysical data the lower layer of sediments (below 7 km) is present only in the central part of Filchner-Ronne Ice Shelf and Lambert Rift (Fig. 3c). The thickness of the lower layer of sediments changes from 0 km near the borders to 5 km in the center of the Filchner-Ronne Basin, with moderate continuation into Southern Weddell Sea. In Lambert Rift, 1-2 km of lower sediments lie from Prydz Bay to Mawson Escarpment. In Ross Sea, this layer is mainly present in the Victoria Land Basin along the Transantarctic Mountains (~1 km). For other marginal seas this sedimentary layer is not found.

3.3 Sediment velocity model

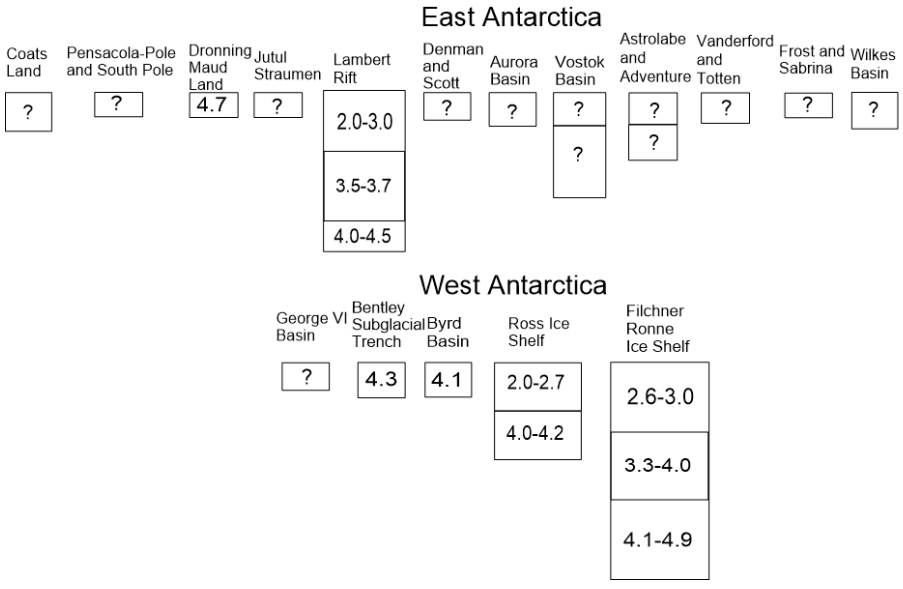

Fig. 4. The average P-wave velocity diagrams for sedimentary basins in Antarctica.

In CRUST1.0, the P-wave velocity in the upper sediments is 3.2 km/s for all Antarctica, except under Ross and Filchner-Ronne Ice Shelves where it is from 1.8 to 2 km/s. Compared to CRUST1.0, our new ANTASed-II model reveals more detail in the

pattern of seismic velocity for the upper sedimentary layer. The P-wave velocity diagrams for the sediments in our model is shown in Fig. 4. The upper sedimentary layer has large velocity variations from 2.0-3.0 km/s for young sediments (Ross Basin) to 4.1- 4.7 km/s for parts of Beacon Supergroup (Dronning Maud Land, Byrd, Bentley basins).

In the middle sedimentary layer of CRUST1.0, P-wave velocity has large variations: from 3.3 km/s for Ronne, Ross and Lambert basins, to 4.6 km/s for the area between Marie Byrd Land and Transantarctic Mountains and for Wilkes Basin. In the Pole area and Aurora Basin it is 4.0 km/s. In our model middle sedimentary layer P-wave velocity also has significant variations: from 3.3-4.0 km/s in Filchner-Ronne Basin to 4.0-4.2 km/s in Ross Basin (Fig.4). Lambert Rift has intermediate velocity in the second sedimentary layer of 3.5-3.7 km/s. In our model, the sediment thickness for the Pole basin does not exceed 2 km and therefore the middle sedimentary layer here is absent.

In the lower sedimentary layer of CRUST1.0, P-wave velocity is about 5 km/s in the area between Marie Byrd Land and Transantarctic Mountains, although — according to the thickness of sediments in CRUST1.0 being less than 7 km — there is no lower layer in this area. In our model the lower sedimentary layer is present only in the Filchner Ronne Ice Shelf and Lambert Rift with P-wave velocity of (4.1 -4.9 km/s) and (4.0-4.5) respectively (Fig. 4).

3.4 Sediment density model

We found density in sedimentary layers using an empirical relation between the P-wave velocity and density from Brocher (2005):

$$\rho\ (g/cm^3) = 1.6612Vp - 0.4721V^2p + 0.0671\ V^3p - 0.0043\ V^4p + 0.000106\ V^5p. \quad (3)$$

507 Equation (3) is the Nafe–Drake curve. It was previously published only graphically
508 (Ludwig et al., 1970) and has been converted to a formula by Brocher (2005).
509 According to this formula the sediment density in Antarctica varies in a wide range,
510 from 1860 kg/m^3 for young Cenozoic sediments in the Ross basin, to 2490 kg/m^3 for
511 old and dense Paleozoic sediments belonging to Beacon Supergroup. The thickness
512 and density of consolidated crustal layers are summarized in Table 2.
513

Sedimentary basin	Total thickness ,km	Upper layer, km	Middle layer, km	Lower layer, km	Upper layer, density (kg/m^3)	Middle layr, density (kg/m^3)	Lower layer, density (kg/m^3)	Origin
Coats Land	1-3	1-2	0-1	-	?	?	-	Rifted sediments in deep trenches
Western Dronning Maud Land	1-2	1-2	-	-	2490	-	-	Beacon Supergroup
Jutulstraumen Rift	1	1	-	-	?	-	-	Rifted sediments?
Lambert Rift	2–9	2	0–7	02	2300-2320	2320–2350	2400-2470	From Devon to Cenozoic rifted sediments
Scott and Denman rifts	1-2	1-2	0	-	?	-	-	Rifted sediments
Vostok Basin	2-6	2	2-4	-	?	?	-	Rifted sediments
Aurora Basin	1-3	1-2	0-1	-	?	?	-	Rifted sediments?
Adventure Trench	2-4	2	0-2	-	?	?	-	Rifted sediments?
Astrolabe Subglacial Basin	2-4	2	0-2	-	?	?	-	Rifted sediments?
Frost Subglacial Basin	1-2	1-2	0	-	?	-	-	Rifted sediments?
Vanderford and Totten rifts	1-2	1-2	0	-	?	-	-	Rifted sediments?
Sabrina Subglacial	1-2	1-2	0	-	?	-	-	Rifted sediments?

Basin								
Wilkes Subglacial Basin	1-3	1-2	0-1	-	?	?	-	Beacon Supergroup, Cenozoic marine sediments?
Ross Ice Shelf	2-6	2	0-4	-	1860-2060	2420	-	Part of West Antarctic Rift System, Mesozoic-Cenozoic sediments in the upper layer, Beacon Supergroup in the lower layer
Byrd and Bentley Subglacial basins	2-4	2	0-2	-	2410	2420-2430	-	Part of West Antarctic Rift System, Beacon Supergroup
Filchner-Ronne Basin	2-12	2	0-5	0-7	2120-2220	2280-2390	2480-2520	Sediments of terrigenous, marine and glacial marine origin in the upper and middle layer, Beacon Supergroup in the lower layer
Pensacola-Pole Subglacial Basin	1-2	1-2	-	-	?	-	-	Beacon Supergroup?
South-Pole Subglacial Basin	1-2	1-2	-	-	?	-	-	Beacon Supergroup?
George VI Basin	1-2	1-2	-	-	?	-	-	Cenozoic rifting, Fossil Bluff Group, sediments of glacial marine origin

514 **Table 2.** Thickness, density and origin of sedimentary basins.

515

516 **4. Discussion and concluding remarks**

517 In this study we considerably improve the previous ANTASed model in several key
518 regions, and delineate new sedimentary basins: George VI in West Antarctica; South
519 Pole, Frost and Sabrina subglacial basins in East Antarctica (Australo-Antarctica block).
520 The boundaries and depths of other sedimentary basins have been clarified. We also
521 merge the GlobSed and the improved ANTASed-II sediment thickness grids, and
522 construct the inner sediment structure for each sedimentary basin.

523 The differences between our new ANTASed-II sediment model (this study) and the
524 previous ANTASed model (Baranov et al., 2021) is −6/+5 km (mean -0.1 km, standard

deviation 0.73 km, see Figure 2b). The combined sediment model that we construct for the continent and the surrounding South Ocean differs significantly (-3 /+11 km) from CRUST1.0 (Fig. 2b).

In addition to significant differences within the continent, rather large differences are also revealed for the seas surrounding continental Antarctica. The greatest differences between our sediment model and CRUST1.0 are found for the southern part of the Weddell Sea. Here our new combined model shows large differences in sediment thickness compared to CRUST1.0 (up to 8 km). The rest of the coastal seas are also characterized by significant excess of the sediment thickness in the new model (up to 4 km). At the same time for some seas, the sediment thickness in the new model is less than in the CRUST1.0 model (up to 3 km).

Geophysical data show the presence of sediments related to a wide range of epochs: from Devonian to Cenozoic deposits. There are numerous factors controlling sediment distribution and properties. Part of sedimentary basins in Antarctica belong to the Beacon Supergroup — connected to sedimentation on the Pacific edge of Gondwana — the other part includes sedimentary basins of rift origin. These basins began to form during the Gondwana breakup; for part of the West Antarctica, rifting continues to the present.

Some sedimentary basins of Antarctica have extensions in the surrounding seas, and receive significant contributions to their sedimentation today. For them, sediments are carried out into the sea and thus they can be studied directly (e.g. Whitehead et al., 2006). Other basins are intracontinental (South Pole, Astrolabe, Adventure, Aurora, Frost, Sabrina and Vostok basins of Australo-Antarctica block).

The distribution of sediments over the basins, as well as their properties, is uneven. There are sedimentary basins with a rather flat relief — Ross, Filchner- Ronne,

western and eastern Dronning Maud Land, South Pole and Pensacola-Pole basins with continuations to the ocean. These basins belong to Beacon Supergroup. The rest of the sediments are located in deep depressions of probably rift origin on the continent. Some of them have access to the sea through which the sediments have been carried out to sea before glaciation. Others lie in a landlocked intercontinental realm. However, here it should be taken into account that the paleotopography before and during the glaciation was very different from the modern bedmap relief (e.g. Wilson and Luyendyk, 2009).

We find several intracontinental depressions inside the continent. According to the subglacial relief (BEDMACHINE, Morlighem et al., 2020), Antarctica is the continent with deepest intracontinental depressions on land that are filled by ice. These are the Bentley and Byrd depressions in West Antarctica, reaching depth up to 2000 m below sea level; the Lambert Rift in East Antarctica; the recently discovered narrow Denman depression with a maximum depth of about 3000 m below sea level on the border of Indo-Antarctica; the Australo-Antarctica blocks of East Antarctica; and some others. At the same time, for the Byrd and Bentley depressions, according to seismic profiles, the sediment thickness is about 2-3 km, which is significantly less than for the Lambert Rift and less than the thickness of sediments in the central part of Filchner-Ronne Ice Shelf, despite the fact that Byrd and Bentley depressions are much deeper. The Byrd and Bentley subglacial depressions certainly have a rift origin but contain dense sediments of presumably Paleozoic age from the Beacon Supergroup. The absence of a significant layer of young sediments for the Bentley and Byrd depressions indicates that their formation probably began after the glaciation of this area of Antarctica.

Lambert Rift has a complex structure. The eastern branch is not very pronounced in the subglacial relief and is well compensated by sediments—

apparently, rifting has stopped long time ago. The western branch of the Lambert Rift is strongly uncompensated, bedrocks lie up to 2000 m below sea level, which means that rifting continued after the glaciation. The bedrock topography is highly contrasting, from a deep depression to the Prince Charles Mountains on the western edge of the Lambert Rift. The Mawson Escarpment between West and East continues towards Prydz Bay under sedimentary cover.

We believe that a similar situation exists in other deep depressions identified by the BEDMACHINE bedrock model, where seismic data are absent: deep trenches bordering the Filchner Ronne Ice Shelf, in the Coats Land, Denman, Scott, Vanderford and Totten depressions, deep grabens of Wilkes Basin with depth in excess of 2 km below sea level. The origin of such deep, narrow, depressions filled by ice can be explained by the continuing rifting after the glaciation of these areas, when sedimentation had already ceased. In the same time the main sedimentation for the Vostok Basin and Filchner Ronne Ice Shelf appears to have occurred prior to glaciation. This fact can be well explained by the ongoing activity of West Antarctic Rift System after glaciation in the Miocene till the present days. The presence of narrow and deep depressions for East Antarctica (Denman, Scott, Wilkes, Vanderford and Totten, Lambert, Coats) and for the border of the Filchner-Ronne Ice Shelf near Coats Land shows that extension could have continued after the glaciation of these parts of Antarctica. Hence parts of East Antarctic Rift System were active after Miocene too. We conclude that narrow subglacial depressions in West and East Antarctica continued to form after glaciation and they practically did not fill with sediments since that time. When approaching the coastline from the land side, the relief of deep depressions quickly flattens out. This can be explained by the periodic regression and transgression of the sea. With local warming and melting of ice near the coast, the

600 subglacial depression is flooded by the sea, and sediments quickly deposit in a deep
601 depression. Closer to the center of the continent, ice has been preserved since the
602 moment of glaciation, preventing deep depressions from filling with sediments.

603 The upper sediment layer is included in all sedimentary basins with thickness less
604 than 2 km. Below 2 km we use the middle sediment layer to describe sediment
605 deposits down to the depth of 7 km, and an additional lower layer for sedimentary
606 basins where thickness exceeds 7 km. The seismic velocity of sediments also has
607 significant variations. We suggest that velocity larger than 4 km/s marks old Paleozoic
608 sediments from the Beacon Supergroup, while Mesozoic sediments have intermediate
609 velocity (3.4-3.7 km/s), and young Cenozoic sediments have velocity of 2.0-3.0 km/s
610 (upper layers of Ross and Filchner Ronne basins). West Antarctica contains young,
611 rifted sediments (upper layer of Ross Ice Shelf basin, 2.0-2.7 km/s; upper layer of
612 Filchner Ronne Ice Shelf, 2.6-3.0 km/s; George VI Basin) and more dense sediments
613 (Byrd, Bentley, lower layers of Ross and Filchner-Ronne basins).

614 The Indo-Antarctica block of East Antarctica has rather high subglacial relief
615 (Morlighem et al., 2020). For this block there are two types of sedimentary basins:
616 deep rifted depressions (JutulStraumen Rift and Lambert Rift, 3.5-3.7 km/s) and more
617 vast basins that belong to Beacon Supergroup having high seismic velocities (Dronning
618 Maud Land basins, 4.7 km/s; Pensacola-Pole Basin, South Pole Basin). The Australo-
619 Antarctica block of East Antarctica is characterized by rather low subglacial relief
620 (Morlighem et al., 2020) and East Antarctic Rift System (Aitken et al., 2014; Frederick
621 et al., 2016; Baranov et al., 2020). There are rifted depressions filled by sediments
622 with unknown velocities (Scott and Denman rifts; Vostok depression; Aurora Basin;
623 Adventure Trench; Astrolabe Basin; Frost and Sabrina basins, Vanderford and Totten
624 rifts and Wilkes basin). These results confirm a significant contrast between the deep

structure of West Antarctica, Indo-Antarctica and Australo-Antarctic blocks of East Antarctica.

Despite the extremely small amount of original seismic data, we observe some regional details in P-wave velocities and maps of the sedimentary layers that are absent in CRUST1.0 and CRUST2.0 models (Fig 3, 4). We find large variations in sediments properties and origin for Antarctica using geophysical data and sufficiently improved three-layer sediment CRUST1.0 model for this region. Nevertheless, new data are still needed particularly for Australo-Antarctica block.

5. Acknowledgments

We thank Professor Walter D. Mooney, the Editor and an anonymous Reviewer for constructive comments which helped to improve the manuscript.

References

Agostinetti, P., Roselli, P., Cattaneo, M., Amato, A., 2005. Moho-depth and subglacial sedimentary layer thickness in the Wilkes Basin from Receiver Function Analysis. IASPEI. General Assembly, October 2.9, 2005, Chile, Abstracts Volume, pp. 281–284.

Aitken, A. R. A., D. A. Young, F. Ferraccioli, P. G. Betts, J. S. Greenbaum, T. G. Richter, J. L. Roberts, D. D.Blankenship, and M. J. Siegert., 2014. The subglacial geology of Wilkes Land, East Antarctica. Geophys. Res. Lett. 41, 2390–2400.

Baranov, A., 2010. A new crustal model for Central and Southern Asia. Izvest Phys Solid Earth 46:34–46.

Baranov, A., Morelli, A., 2013. The Moho depth map of the Antarctica region. Tectonophysics 609:299–313.

650 Baranov, A., Tenzer, R., and Bagherbandi, M., 2018a. Combined Gravimetric-Seismic
651 Crustal Model for Antarctica. Surv. Geophys. 39, 23–56. doi:10.1007/s10712-
652 017-9423-5
653 Baranov, A., Bagherbandi, M., and Tenzer, R., 2018b. Combined Gravimetric-Seismic
654 Moho Model of Tibet. Geosciences 8, 461. doi:10.3390/geosciences8120461
655 Baranov, A., Tenzer, R., and Morelli, A., 2021. Updated Antarctic Crustal Model,
656 Gondwana Res. 89, 1–18. doi:10.1016/j.gr.2020.08.010
657 Baranov, A., Morelli, A., Chuvaev A., 2021. ANTASed – An Updated Sediment Model for
658 Antarctica. Front. Earth Sci. 9:722699. doi: 10.3389/feart.2021.722699
659 Bassin, C., Laske, G., Masters, G., 2000. The current limits of resolution for surface
660 wave tomography in North America. EOS. Transactions of the American
661 Geophysical Union 81.
662 Beaudoin, B.C., ten Brink, U.S., Stern, T.A., 1992. Characteristics and processing of
663 seismic data collected on thick, floating ice: results from the Ross Ice Shelf,
664 Antarctica, Geophysics 57, 1359–1372.
665 Behrendt, J. C., 1999. Crustal and lithospheric structure of the West Antarctic Rift
666 System from geophysical investigations: a review. Glob. Planet. Change 23,
667 25–44.
668 Bentley, C., 1973. Crustal structure of Antarctica. Tectonophysics 20, 229–240.
669 Bell, A. C., King, E. C., 1998. New seismic data support Cenozoic rifting in George VI
670 Sound, Antarctic Peninsula. Geophysical Journal International, 134(3), 889–
671 902. https://doi.org/10.1046/j.1365-246x.1998.00605.x
672 Bobrov, A., M., Baranov A., A., 2018. Modeling of moving deformable continents by
673 active tracers: closing and opening of oceans, recirculation of oceanic crust.
674 Geodynamics & Tectonophysics, 9 (1), 287–307. DOI: 10.5800/GT-2018-9-1-

675 0349.
676 Boger, S., Wilson, C., 2003. Brittle faulting in the Prince Charles Mountains, East
677 Antarctica: cretaceous transtensional tectonics related to the break-up of
678 Gondwana, Tectonophysics, 367 173–186.
679 Brocher T.M., 2005. Empirical relations between elastic wavespeeds and density in the
680 Earth's crust. Bull. Seismol. Soc. Amer., 95, 6, 2081-2092.
681 Chuvaev, A., Baranov, A., Bobrov, A., 2020. Numerical modelling of mantle convection
682 in the Earth using cloud technologies, Computational Technologies 25(2) 103–
683 118.
684 Crabtree, R. D., Storey, B. C., & Doake, C. S. M. 1985. The structural evolution of
685 George VI Sound, Antarctic Peninsula. Tectonophysics, *114*(1–4), 431–442.
686 https://doi.org/10.1016/0040-1951(85)90025-3
687 Danesi S., and A. Morelli, 2001. Structure of the upper mantle under the Antarctic
688 Plate from surface wave tomography, Geophys. Res. Lett., 28, 4395-4398.
689 Davey, F. J., S. C. Cande, Stock, J. M., 2006. Extension in the western Ross Sea region-
690 links between Adare Basin and Victoria Land Basin, Geophys. Res. Lett. 33
691 L20315
692 Divins, D., 2003. Total sediment thickness of the world's oceans and marginal seas.
693 Boulder, CO: NOAA National Geophysical Data Center.
694 Fedorov, L.V., Grikurov, G.E., Kurinin, R.G., Masolov, V.N., 1982. Crustal structure of
695 the Lambert Glacier area from geophysical data. In: Craddock, C. (Ed.),
696 Antarctic Geoscience. Univ. of Wisconsin Press, Madison, pp. 931–936.
697 Frederick, B.C., Young, D.A., Blankenship, D.D., Richter, T.G., Kempf, S.D., Ferraccioli.
698 F., Siegert, M.J., 2016. Distribution of subglacial sediments across the Wilkes

699 Subglacial Basin, East Antarctica, J Geophys Res Earth Surf 121, 790–813,790–
700 813. doi:10.1002/2015jf003760
701 Huang, X., Gohl, K., Jokat, W., 2014. Variability in Cenozoic sedimentation and
702 paleowater depths of the Weddell Sea basin related to pre-glacial and glacial
703 conditions of Antarctica. Global and Planetary Change 118, 25–41.
704 https://doi.org/10.1016/j.gloplacha.2014.03.010.
705 Hübscher, C., Jokat, W., Miller, H., 1996. Structure and origin of the Earth's crust in the
706 southern Weddell Sea - results and implications. In: Storey, B.C., King, E.C.,
707 Livermore, R.A. (Eds.), Weddell Sea Tectonics and Gondwana Break-up 108.
708 Geological Society Special Publication, pp. 201–211.
709 http://dx.doi.org/10.1144/GSL.SP.1996.108.01.15.
710 Hungeling, A., Tyssen, F., 1991. Reflection seismic measurements in western
711 Neuschwabenland. In: Thornson MRA, Crame JA, Thomson JW (eds)
712 Geological evolution of Antarctica. Proceedings of the fifth international
713 symposium on Antarctic Earth Sciences, Robinson College, Cambridge,
714 Cambridge University Press, Cambridge, UK, p 73.
715 Isanina, E., Krupnova, N., Popov, S., Masolov, V., Lukin, V., 2009. Deep structure of the
716 Vostok Basin, East Antarctica as deduced from seismological observations.
717 Geotektonika, 3, 45–50.
718 Ji, F., Li, F., Gao, J.-Y., Zhang, Q., Hao, W.-F., 2018. 3-D density structure of the Ross Sea
719 basins, West Antarctica from 422 constrained gravity inversion and their
720 tectonic implications. Geophysical Journal International 215, 1241-1256. 423
721 10.1093/gji/ggy343424
722 Jokat, W., Herter, U., 2016. Jurassic failed rift system below the Filchner-Ronne-Shelf,
723 Antarctica: New evidence from geophysical data, Tectonophysics, 688, 65-83.

724 Kanao, M.; Fujiwara, A.; Miyamachi, H.; Toda, S.; Tomura, M.; Ito, K.; Ikawa, T.
725 Reflection imaging of the crust and the lithospheric mantle in the Lützow–
726 Holm Complex, Eastern Dronning Maud Land, Antarctica, derived from the
727 SEAL Transects. Tectonophysics 2011, 508, 73–84.
728 Kurinin, R.G., Grikurov, G.E., 1982. Crustal structure of part of East Antarctica from
729 geophysical data, in: C. Craddock (Ed.), Antarctic Geoscience, University of
730 Wisconsin Press, Madison, pp. 895–901.
731 Kolmakov, A., Mishenkin, B., Solovyev, D., 1975. Deep seismic studies in East
732 Antarctica. Bull. Soviet Antarc. Exped. 5–15 (in Russian).
733 Laske, G., Masters, G., 1997. A global digital map of sediment thickness. Eos,
734 Transactions American Geophysical Union 78, F483.
735 Laske, G., Masters, G., Ma, Z., Pasyanos, M.E., 2013. Update on CRUST1.0—A 1-degree
736 global model of Earth's crust. Geophys Res Abstr 15:2658.
737 Leitchenkov, G., Kudryavtzev, G., 1997. Structure and origin of the Earth's Crust in the
738 Weddell Sea Embayment (beneath the Front of the Filchner and Ronne Ice
739 Shelves) from deep seismic sounding data, Polarforschung, 67,3 143–154.
740 Lindeque, A., Gohl, K., Wobbe, F., & Uenzelmann-Neben, G., 2016. Preglacial to glacial
741 sediment thickness grids for the Southern Pacific Margin of West Antarctica.
742 Geochemistry, Geophysics, Geosystems, 17, 4276–4285.
743 https://doi.org/10.1002/2016GC006401
744 Lisker, F., Brown, R., Fabel, D., 2003. Denudation and thermal history along a transect
745 across the Lambert Graben, northern Prince Charles Mountains, Antarctica,
746 derived from apatite fission track thermochronology. Tectonics, 22, 1055.
747 Lucas, E., M., Soto, D., Nyblade, A., A., Lloyd, A., J., Aster, R. C., Wiens, D.,
748 A., O'Donnell, J., P., Stuart, G., W., Wilson, T., J., Dalziel, I., W., Winberry,

J., P., Huerta, A., D. , 2020. P- and S-wave velocity structure of central West Antarctica: Implications for the tectonic evolution of the West Antarctic Rift System, Earth and Planetary Science Letters 546 116437.

Ludwig, W. J., J. E. Nafe, and C. L. Drake., 1970. Seismic refraction, in The Sea, A. E. Maxwell (Editor), Vol. 4, Wiley-Interscience, New York, 53–84.

Maslanyj, M. P., 1988. Gravity and aeromagnetic evidence for the crustal structure of George VI Sound, Antarctic Peninsula. British Antarctic Survey Bulletin, *79*, 1–16.

McGinnis, L.D., Bowen, R.H., Erickson, J.M., Allred, B.J., Kreamer, J.L., 1985. East-West Antarctic boundary in McMurdo Sound. Tectonophysics 114, 341–356.

Morelli A., and S. Danesi, 2004. Seismological imaging of the Antarctic continental lithosphere: a review, Global Planet. Change, 42, 155-165.

Morlighem, M., Rignot, E., Binder, T., Blankenship, D., Drews, R., Eagles, G., Eisen, O., Ferraccioli, F., Forsberg, R., Fretwell, P., et al. (2020). Deep glacial troughs and stabilizing ridges unveiled beneath the margins of the Antarctic ice sheet, Nat. Geosci 13 132–137.

Munson, C.G., Bentley, C.R., 1992. The crustal structure beneath ice stream C and ridge BC, West Antarctica from a seismic refraction and gravity profile. In: Yoshida Y,

Kaminuma K, Shiraishi K (eds) Recent progress in Antarctic earth science, TERRAPUB, Tokyo 507–514.

Rooney, S.T., Blankenship, D.D., Bentley, C.R., 1987. Seismic refraction measurements of crustal structure in West Antarctica, In: McKenzie GD (ed) Gondwana Six: structure, tectonics and geophysics, Geophysical Monograph Series 40 1–7.

773 Scheinert, M., Ferraccioli, F., Schwabe, J., Bell, R., Studinger, M., Damaske, D.,
774 Jokat,W., Aleshkova, N., Jordan, T., Leitchenkov, G., Blankenship, D. D.,
775 Damiani, T.M.,
776 Young, D., Cochran, J. R., Richter, T. D., 2016. New Antarctic gravity anomaly grid for
777 enhanced geodetic and geophysical studies in Antarctica, Geophys. Res. Lett.
778 43 600–610.
779 Snyder, John P.; Voxland, Philip M., 1989. An Album of Map Projections. Professional
780 Paper *1453.* Denver: USGS. *p. 228.* ISBN 978-0160033681.
781 Sobolev A.V., Hoffman A.W., Kuzmin D.V., Yaxley G.M., Arndt N.T., Chung S-L.,
782 Danyushevsky L.V., Elliott T., Frey F.A., Garcia M.O., Gurenko A.A.,
783 Kamenetsky V.S., Kerr A.C., Krivolutskaya N.A., Matvienkov V.V., Nikogosian
784 I.K., Rocholl A., Sigurdsson I.A., Sushchevskaya N.N., Teklay M., 2007. The
785 amount of recycled crust in sources of mantle-derived melts. Science 316
786 (5823), 412–417. https://doi.org/10.1126/science.%201138113
787 Straume, E.O., Gaina, C., Medvedev, S., Hochmuth, K., Gohl, K., Whittaker, J. M., et al.
788 (2019). GlobSed: Updated total sediment thickness in the world's oceans,
789 Geochemistry, Geophysics, Geosystems 20.
790 ten Brink, U.S., Beaudoin, B.C., Stern, T.A., 1993. Geophysical investigations of the
791 tectonic boundary between East and West Antarctica, Science 261 45–50.
792 Trey, H., Cooper, A., Pellis, G., della Vedova, B., Cochrane, G., Brancolini, G., Makris, J.,
793 1999. Transect across the West Antarctic rift system in the Ross Sea,
794 Antarctica. Tectonophysics 301:61–74.
795 Trubitsyn, V., Baranov, A., Kharybin E., 2007. Numerical Models of Subduction of the
796 Oceanic Crust with Basaltic Plateaus. Izvestiya, Physics of the Solid Earth
797 43(7), 533-542. http://dx.doi.org 10.1134/S1069351307070014

798 Whitehead, J.M., Quilty, P.G., Mckelvey, B.C., O'Brien, P.E., 2006. A review of the
799 Cenozoic stratigraphy and glacial history of the Lambert Graben–Prydz Bay
800 region, East Antarctica. Antarctic Science 18 83–99.
801 Whittaker, J. M., Goncharov, A., Williams, S. E., Müller, R. D., & Leitchenkov, G., 2013.
802 Global sediment thickness data set updated for the Australian-Antarctic
803 Southern Ocean. Geochemistry, Geophysics, Geosystems, 14, 3297–3305.
804 https://doi.org/10.1002/ggge.20181
805 Wessel, P., Luis, J. F., Uieda, L., Scharroo, R., Wobbe, F., Smith, W. H. F., & Tian, D.,
806 2019. The Generic Mapping Tools version 6. Geochemistry, Geophysics,
807 Geosystems, 20, 5556–5564. https://doi.org/10.1029/2019GC008515
808 Wilson, D.S., Luyendyk, B.P., 2009. West Antarctic paleotopography estimated at the
809 Eocene–Oligocene climate transition. Geophys. Res. Lett. 36 (16), L16302.
810 http://dx.doi.org/10.1029/2009GL039297.
811 Wobbe, F., Lindeque, A., & Gohl, K., 2014. Anomalous South Pacific lithosphere
812 dynamics derived from new total sediment thickness estimates off the West
813 Antarctic margin. Global and Planetary Change, 123, 139–149.
814 https://doi.org/10.1016/j.gloplacha.2014.09.006